

# Imperfect Mixing in Continuous Flow Stirred-Tank Reactors

R. C. AGGARWAL and F. S. MANNING

University of Tulsa, Tulsa, Oklahoma

Recently Patel (4) studied imperfect mixing in steady state continuous flow stirred-tanks by feeding freshwater into a tank initially filled with salt water and monitoring the concentration of the exit stream. Patel's data covered the following ranges:

Type of agitator = six-blade paddle impeller and  
marine propeller  
Agitator diameter = 2.5 to 4.0 in.  
Rotational speed = 0 to 100 r.p.m.  
Dilution rate = 0.09 to 0.126 min.<sup>-1</sup>

Hubbard and Patel (1) presented an extensive dimensional analysis of imperfect mixing and so identified the variables which influence the mixing process most strongly.

This communication shows how the Manning, Wolf, and Keairns model can predict such imperfect mixing processes.

Figure 1a shows a physical picture of Patel's mixing tank, while Figure 1b shows the flow and mixing patterns based on the Manning, Wolf, and Keairns model (2, 3). This model divides the vessel into two zones: the micro-mixer, or a small region surrounding the impeller, which is characterized by violent agitation; and the remaining tank volume where mixing is comparatively mild. The mixing in the first zone is assumed perfect even down to the microlevel, while only macroscale mixing occurs in the second zone.

A material balance on the whole tank yields

$$\text{Accumulation of salt} = \text{Flow input} - \text{Flow output} \quad (1)$$

$$= F C_F - F C_{\text{exit}}$$

However, the fluid in the tank consists of fresh unmixed feed which has not yet passed through the mixer and recirculating fluid which has passed through the mixer. The relative volumes of the feed and recirculating streams are proportioned according to their flow rates in the macro-mixer. If the micromixer volume is assumed negligible

$$V_T \frac{F}{F+Q} \frac{dC_F}{dt} + V_T \frac{Q}{F+Q} \frac{dC_{\text{macro}}}{dt} = F C_F - F C_{\text{exit}} \quad (2)$$

If the feed  $F$  is freshwater  $C_F = 0$ , Equation (2) becomes

$$\frac{dC_{\text{macro}}}{dt} = - \frac{F}{V_T} \frac{F+Q}{Q} C_{\text{exit}} \quad (3)$$

Figure 1b shows that the discharge stream  $C_{\text{macro}}$  and the vessel exit stream  $C_{\text{exit}}$  concentrations are equal; therefore

$$\frac{dC_{\text{exit}}}{dt} = - \frac{F}{V_T} \left( \frac{F+Q}{Q} \right) C_{\text{exit}} \quad (4)$$

Integrating between  $C_{\text{exit}} = C_{\text{in}}$  at  $t = 0$  and  $C_{\text{exit}} = C_{\text{exit}}$  at  $t = t$ , we get

$$\ln \frac{C_{\text{exit}}}{C_{\text{in}}} = - \frac{F}{V_T} \left( \frac{F}{Q} + 1 \right) t \quad (5)$$

The dilution ratio  $D$ , or reciprocal of average residence

time, is defined by  $F/V_T$ ; therefore

$$\ln \frac{C_{\text{exit}}}{C_{\text{in}}} = - D \left( \frac{F}{Q} + 1 \right) t \quad (6)$$

If the entire tank were assumed to be completely micro-mixed, a total material balance would yield

$$\ln \frac{C_{\text{exit}}}{C_{\text{in}}} = - D t \quad (7)$$

Notice that Equations (6) and (7) differ by only the factor  $F/Q + 1$ . When  $Q$  is large compared to  $F$  (that is, vigorous mixing) the factor  $F/Q + 1$  is nearly 1 and the vessel behaves as if it were perfectly mixed.

If fresh water is fed into a CFST containing salt water, the output stream concentration will not change instantaneously. A small time lag occurs before the fresh water reaches the output port. This time lag may be estimated by the time to circulate the fluid in the tank once, that is,  $V_T/Q$ .

Patel's data (4) on impellers were fitted to the following model:

$$\frac{C_{\text{exit}}}{C_{\text{in}}} = 1 \quad \text{for } 0 \leq t < \frac{V_T}{Q} \quad (8)$$

and

$$\ln \frac{C_{\text{exit}}}{C_{\text{in}}} = - D \left( \frac{F}{Q} + 1 \right) t \quad \text{for } \frac{V_T}{Q} < t \quad (9)$$

In Patel's equipment the impeller discharge flows horizontally and the fluid must therefore circulate through the

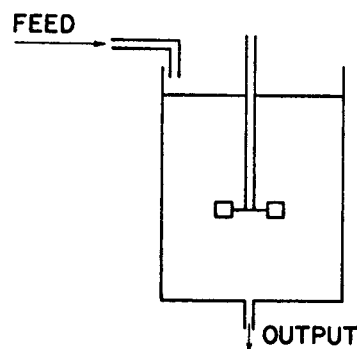


Fig. 1a. Physical picture.

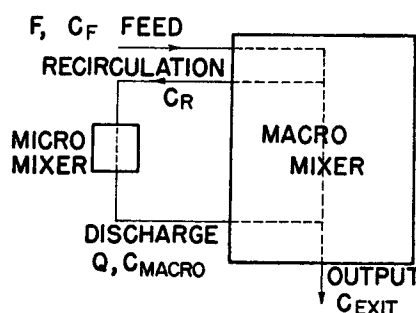


Fig. 1b. Flow and mixing patterns.

TABLE 1. COMPARISON OF PATEL'S DATA AND THE MANNING, WOLF, KEAIRNS MODEL

Run No.	Agitator type	Agitator diam-eter, in.	Agitator, r.p.m.	Q, ml./min.	F/Q, min. <sup>-1</sup>	V <sub>T</sub> , ml.	Dilution ratio D, min. <sup>-1</sup>	H <sub>1</sub> , in.	H <sub>L</sub> , in.	% Model fit*
1	Impeller	2.5	50	5,900	0.1128	5290	0.126	2.6	7.6	7.65
2	Impeller	2.5	25	2,950	0.227	5290	0.127	2.6	7.6	10.0
3	Impeller	2.5	10	1,180	0.565	5290	0.126	2.6	7.6	34.7
4	Propeller	2.5	75	10,400	0.064	5290	0.126	2.6	7.6	11.5
5	Propeller	2.5	50	6,930	0.0998	5290	0.125	2.6	7.6	9.0
7	Impeller	2.5	50	5,900	0.1128	5290	0.126	3.6	7.6	7.8
8	Impeller	2.5	25	2,950	0.225	5290	0.126	3.6	7.6	14.2
9	Propeller	3.0	50	12,000	0.0552	5290	0.125	3.6	7.6	16.74
10	Propeller	3.0	25	6,000	0.111	5290	0.126	3.6	7.6	12.18
11	Impeller	2.5	100	11,800	0.0492	6280	0.0922	4.2	9.0	1.13
12	Impeller	2.5	50	5,900	0.0984	6280	0.0922	4.2	9.0	10.3
13	Impeller	2.5	25	2,950	0.1965	6280	0.0924	4.2	9.0	50.5
14	Propeller	2.5	100	24,000	0.022	6280	0.0919	4.2	9.0	3.3
15	Propeller	2.5	50	6,940	0.084	6280	0.0926	4.2	9.0	36.3
16	Propeller	2.5	25	3,470	0.1665	6280	0.092	4.2	9.0	39.5
17	Impeller	3.0	100	20,400	0.0285	6280	0.0926	4.2	9.0	3.2
18	Impeller	3.0	50	10,200	0.057	6280	0.0924	4.2	9.0	7.6
19	Impeller	3.0	10	2,040	0.283	6280	0.0917	4.2	9.0	39.0
21	Propeller	3.0	100	24,000	0.022	6280	0.0919	4.2	9.0	4.7
22	Propeller	3.0	50	12,000	0.0475	6280	0.0909	4.2	9.0	28.2
23	Propeller	3.0	25	6,000	0.0935	6280	0.0892	4.2	9.0	32.4
25	Impeller	4.0	25	12,100	0.0471	6280	0.0906	4.2	9.0	2.2
26	Impeller	4.0	10	4,850	0.117	6280	0.0904	4.2	9.0	31.0
27	Propeller	4.0	50	28,400	0.0201	6280	0.0908	4.2	9.0	6.6
28	Propeller	4.0	25	14,200	0.0407	6280	0.0920	4.2	9.0	9.6
29	Propeller	4.0	10	5,680	0.1018	6280	0.0920	4.2	9.0	60.4
31	Impeller	4.0	50	24,200	0.0236	6280	0.0908	4.2	9.0	1.86

\* The deviation between Patel's exit concentration data and the Manning, Wolf, Keairns model predictions,  $[\Sigma(C_{MWK} - C_P)/C_P]/n$ .

vessel before it reaches the exit port situated at the bottom wall. However in Patel's data on propellers the propeller discharge is aimed directly at the exit port, but the overall recirculating flow patterns within the vessel exhibit a stagnation point at the exit port. This stagnation point accounts for the time lag.

Table 1 summarizes the results of modeling Patel's data with Equations (9) and (10). Pumping capacities were

estimated using Wolf and Manning's correlations (5): for flat-bladed turbine impellers  $Q = 2.3 N D_i^2 d$ , while for standard marine propellers:  $Q = 0.54 N D_i^3$ . Figure 2 shows a typical fit.

Comparison of Patel's data with the Manning, Wolf, and Keairns model supports the following conclusions:

1. Model predictions agree closely with Patel's data when  $F/Q$  is less than 0.2, that is, when the impeller discharge dominates the mixing process.

2. Significant deviations occur at very low rotational speeds, that is, when the inlet and exit flows to and from the vessel control the circulation patterns. The Manning, Wolf, and Keairns model does not apply to this model.

3. The Manning, Wolf, and Keairns model is very convenient. The only information required is design data such as tank size, impeller type, size, and rotational speed. Because of these factors the Manning, Wolf, and Keairns model can be used for design purposes such as scaleup.

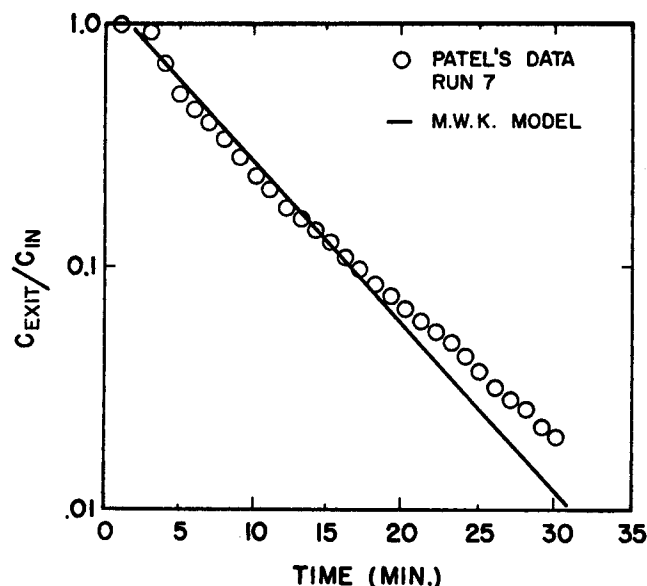


Fig. 2. Typical comparison of the Manning, Wolf, and Keairns model with Patel's data.

#### NOTATION

- $C_F$  = feed concentration
- $C_{exit}$  = output stream concentration
- $C_{macro}$  = impeller discharge concentration
- $C_R$  = recirculation stream concentration as it enters the impeller
- $C_{in}$  = initial concentration in the tank
- $C_{MWK}$  =  $C_{exit}/C_{in}$  as predicted by Manning, Wolf, Keairns model
- $C_P$  =  $C_{exit}/C_{in}$  as measured by Patel
- $D$  = dilution ratio =  $Q/V_T \text{ min.}^{-1}$

$D_i$  = diameter of the impeller  
 $d$  = impeller blade width  
 $F$  = feed flow rate  
 $N$  = impeller speed  
 $n$  = number of data points for any run  
 $Q$  = impeller pumping capacity  
 $t$  = time  
 $V_T$  = volume of stirred tank  
 $H_i$  = height of impeller from the bottom of mixing tank  
 $H_L$  = height of liquid level in the mixing tank

## LITERATURE CITED

1. Hubbard, D. W., and H. Patel, paper presented at AIChE 62nd Ann. Meeting, Washington, D. C. (Nov. 1969).
2. Kearns, D. L., and F. S. Manning, *AIChE J.*, **15**, 660 (1969).
3. Manning, F. S., D. Wolf, and D. L. Kearns, *ibid.*, **11**, 723 (1965).
4. Patel, H., M. S. thesis, Michigan Technol. Univ. (1968).
5. Wolf, D., and F. S. Manning, *Can. J. Chem. Eng.*, **137** (June 1966).

# Reduction of Thermal Stratification by Nonuniform Wall Heating

L. B. EVANS, E. S. MATULEVICIUS, and P. C. PAN

Massachusetts Institute of Technology, Cambridge, Massachusetts

The phenomenon of thermal stratification, which occurs when a confined fluid is heated through the sidewalls of its enclosure, has been the subject of a number of recent investigations (1 to 6), and the fundamental mechanisms are well understood. In a thermally stratified fluid an axial temperature distribution is established in the bulk of the fluid, and the temperature at the top can exceed the mixed-mean temperature by a considerable amount. The axial temperature distribution can be predicted (5, 6) with reasonable confidence for well-defined geometries subjected to a uniform sidewall heat flux.

In many engineering applications, particularly those involving storage of cryogenic fluids, thermal stratification is undesirable. A rocket propellant tank, for example, must be designed to withstand the vapor pressure of the warmest liquid in the tank. The extent to which the temperature of the warmest liquid at the surface exceeds the mixed-mean temperature will depend upon the severity of thermal stratification. Several studies (7 to 11) have been undertaken in an effort to develop techniques for reducing thermal stratification, but the methods reported have not been generally successful.

The experiments described here were carried out to determine the effect of a nonuniform sidewall heat flux on the thermal stratification phenomena. A most remarkable effect was observed which may have direct application to the control of thermal stratification.

## EXPERIMENTS

The experimental apparatus (6), shown schematically in Figure 1, was a rectangular cavity 8 in. wide, and 2 ft. deep, filled to a height of 2 ft. with water as the test fluid. The motion of a dye tracer introduced into the water could be observed through transparent front and rear walls. Each sidewall was a Pyrex glass heater evenly coated with a thin electrically con-

ducting film for resistive heating. Each of the sidewall heaters was divided into three 8-in. vertical sections whose heating rate could be adjusted independently. Thermocouples measured the axial temperatures at six vertical positions in the center of the enclosure.

Heat losses from the system were held to a minimum by providing 4 in. of polyurethane foam insulation at the sides and bottom, by using double panes of glass for the front and rear walls, and by coating the free liquid surface with a surfactant film of stearic acid to retard vaporization.

Two experiments will be reported. In the first, the heat flux distribution in the three vertical segments was uniform (with ratios of heat flux in each segment of 1:1:1). In the second, the heat flux decreased with vertical distance up the plate (with ratios of heat flux in each segment of 1:2:3 in the order top:middle:bottom). The total rate of heat input to the system was the same (4,920 B.t.u./hr. at each sidewall) for both experiments. The experimental conditions corresponded to a fluid Prandtl number of 7 and a modified Grashof number

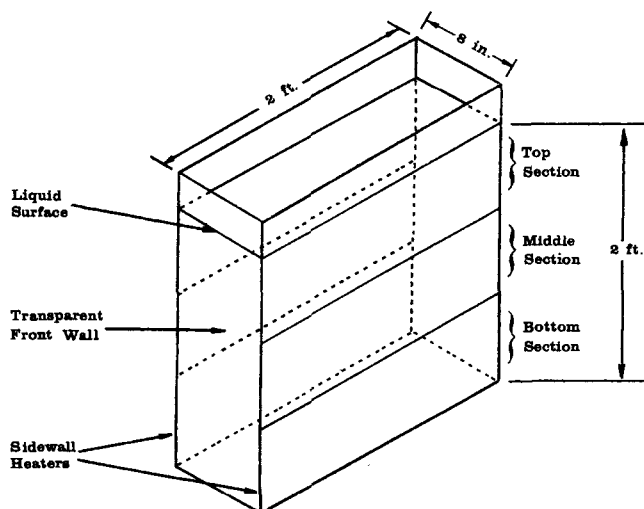


Fig. 1. Schematic diagram of experimental liquid enclosure.

E. S. Matulevicius is with Esso Research and Engineering Company, Linden, New Jersey.